JOURNAL OF APPLIED ELECTROCHEMISTRY 25 (1995) 73–79

Electrocatalytic oxidation of benzyl alcohol in alkaline medium on RuO_2-coated titanium electrode

S.-M. LIN, T.-C. WEN*

Department of Chemical Engineering, National Cheng Kung University, Tainan, Taiwan 70101, Republic of China

Received 8 March 1994; revised 3 June 1994

The heterogeneous electrocatalytic redox behaviour of RuO_2 electrodes fabricated by thermal decomposition is investigated with and without benzyl alcohol using cyclic voltammetric and potentiodynamic techniques. The cyclic voltammetric results show that benzyl alcohol oxidation is mediated by perruthenate ion electrogenerated at the electrode surface. Evaluation of kinetic parameters in relation to Tafel lines allows the postulation of a plausible reaction scheme in which benzyl alcohol adsorbs on the RuO_2 electrode surface and the rate determining step is chemical reaction between perruthenate and adsorbed species. The reaction orders with respect to benzyl alcohol and OH^- concentrations are 0.85 and 1, respectively. The results in galvanostatic electrolysis show that the major product for benzyl alcohol oxidation in an aqueous solution is benzaldehyde, and the organic yield is affected by such electrolysis conditions as *t*-butanol concentration, electrolysis current density, KOH concentration and electrolysis temperature.

1. Introduction

The heterogeneous catalytic oxidation of organic substances by redox catalysis was first explored by previous work [1–3] at nickel (more exactly, NiOOH) electrodes and the application of such redox catalysis for the oxidation of alcohols, aldehydes, amines and related compounds has been extensively reviewed [4]. The reaction mechanism was thought to occur heterogeneously and to involve a rate-determining chemical reaction between a high valent state of the oxide and the adsorbed substance. Further studies concerning heterogeneous redox catalysis electrodes were reported by Beck and Schulz [5–8] who studied the oxidation of a number of organic compounds, especially isopropanol, at titanium/chromium(III) oxide + TiO_2 composite electrodes and found that the Cr^{3+}/Cr^{6+} redox pair possessed considerable activity for organic oxidation. Recently, Ravichandran *et al.* [9–11] studied the electrocatalytic reduction of a series of aromatic compounds at a Ti/ceramic TiO_2 electrodes and found that reduction reactions were catalyzed by the Ti^{4+}/Ti^{3+} redox system. The application of redox catalysis for organic synthesis has, accordingly, received increased attention [12, 13].

Metal oxide coated electrodes, such as ruthenium dioxide (RuO_2), iridium dioxide (IrO_2) etc. are materials that have been widely investigated as electrodes in the chlor-alkali industry and for oxygen evolution [14, 15]. Among them, the RuO_2 electrode possessed various redox pairs in the potential range between the hydrogen and oxygen gas evolution regions [14–17], and is considered to be a good anode for organic synthesis. O'Sullivan and White [18] studied the oxidation of formaldehyde on a RuO_2 electrode and found that formaldehyde was oxidized to formate by ruthenate and then further oxidized to carbonate by perruthenate. Their results were recently elaborated by Lyons *et al.* [19] who reported the transformation of the substrate to the product via a Michaelis–Menten mechanism in the hydrated oxide layer. The electrocatalytic oxidation of alcohols on carbon electrodes modified by polypyrrole-RuO_2 films was studied by Cosnier *et al.* [20, 21]. The results showed that a series of aromatic alcohols were oxidized by the electrogenerated oxidizing species, RuO_4^{2-}, to their corresponding aldehydes or ketones. Recently, we reported that the rate of aniline oxidation on a RuO_2 electrode was higher than that on a platinum electrode and consequently increased the polyaniline growth rate on the former electrode; these results were attributed to a stronger adsorption of aniline on the RuO_2 electrode [22]. Strong adsorption due to weak π-bonding between aromatic species and transition metal oxides is a dominant factor determining electrocatalytic activity [12, 13, 23]. The above information stimulated the present investigation of the electrocatalytic oxidation of benzyl alcohol on thermally prepared RuO_2 electrodes.

In this study, the electrocatalytic oxidation of benzyl alcohol on RuO_2 is first examined by cyclic voltammetry. Kinetic parameters studied by Tafel plots, as well as the effect of galvanostatic electrolysis conditions on benzyl alcohol oxidation current efficiency and benzaldehyde production yield are also presented.

* To whom correspondence should be addressed.

0021-891X

2. Experimental details

2.1. *Preparation of RuO_2 electrode*

RuO_2-coated titanium electrodes were prepared in a manner similar to that reported in previous work [16]. The precursor, $RuCl_3.xH_2O$ (Johnson Matthey, 42.25% metal content), was dissolved in an isopropanol solution containing 10% by volume concentrated HCl, giving a 0.25 M total solution. The titanium (1 cm × 1 cm and 3 cm × 3 cm, for potentiodynamic and galvanostatic electrolysis studies, respectively) supports were first degreased with soap and water, then etched for 1 h in a 3 M HCl solution at 80 to 90° C. A RuO_2 coating was formed by baking the etched plate at 85° C for several minutes after it was dipped in its respective coating solution. After drying, the support was heated under air flow at an annealing temperature of 400° C for 10 min. The entire procedure was repeated seven times after which the support was heated at the annealing temperature for 2 h.

2.2. *Electrochemical studies*

Electrochemical experiments were carried out in a BAS-100B potentiostat/galvanostat system (Bioanalytic System, Inc., USA). An Ag/AgCl electrode (Argenthal, 3 M KCl, 0.207 V vs NHE at 25° C) was used as the reference, while a platinum wire was employed as the counter electrode. A Luggin capillary, whose tip was set at a distance of about 1 mm from the surface of the working electrode, was used to minimize errors due to electrolyte iR drop. All measurements were performed under nitrogen flow and all potentials were quoted vs the Ag/AgCl.

2.3. *Galvanostatic electrolysis*

Galvanostatic electrolysis was carried out in a divided cell with Nafion 435®, a platinum wire, a RuO_2 electrode and an Ag/AgCl electrode as separator, cathode, anode and reference electrode, respectively. The solutions in the anodic and cathodic compartments were 100 cm^3 in volume, stirred by a magnetic bar and separated by a Nafion® cation membrane. The d.c. power was supplied by a HA-301 potentiostat/galvanostat system (Hokuto Denko Company, Japan) and the amount of electricity passed was 0.5 F mol^{-1}. The organic vapour was condensed by a reflux condenser and the reactor was immersed in a water bath controlled at the required temperature with an accuracy of 0.05° C by means of a water thermostat (HAAKE D8 and G).

After electrolysis, 20% *t*-butanol was added to the aqueous anolytic solution to dissolve the products. Samples taken from the anodic compartment were acidified with hydrochloric acid prior to analysis by high performance liquid chromatography (LC-10A, SPD-10A, Shimazu, Japan).

3. Results and discussion

3.1. *Cyclic voltammetry*

Cyclic voltammograms of the RuO_2-coated electrode in 1 M KOH solution without and with the addition of 0.3 M benzyl alcohol at a scan rate of 50 mV s^{-1} are shown in curves 1 and 2, respectively (Fig. 1). In 1 M KOH solution (Fig. 1(a)), a broad peak between −100 and 150 mV (P_1) and a reversible peak (E_p at ca. 320 mV, P_2) are observed. An examination of Fig. 1(a) reveals that, peak P_1 and P_2 exhibit a potential difference in the forward/back scan of $\Delta E < 10$ mV, which is indicative for a process with surface redox states. The oxyruthenium redox transitions, corresponding to P_1 and P_2 in Fig. 1(a), respectively, may be assigned in relatively simple terms as Ru(IV)/Ru(VI), i.e.

$$RuO_2 + 4OH^- \rightleftharpoons RuO_4^{2-} + 2H_2O + 2e^- \quad (1)$$

and Ru(VI)/Ru(VII), i.e.

$$RuO_4^{2-} \rightleftharpoons RuO_4^- + e^- \quad (2)$$

The ruthenium species depicted in the above equations have been written in simple forms, as suggested, either by electrochemical [24] or point of zero charge measurements [25], to be fixed in a thin hydrated layer at the oxide-solution interface. The actual structure of the hydrated surface species was probably complicated, as suggested by measuring the potential-pH dependence for oxyruthenium redox transitions [26].

In the presence of benzyl alcohol in the solution, the anodic current increased considerably at about 150 mV and reached a rising plateau at about 300 mV, indicating that the Ru(VI)/Ru(VII) redox pair possesses catalytic activity for benzyl alcohol oxidation. Accordingly, the mechanism of benzyl alcohol oxidation on RuO_2 involves the participation of oxyruthenium surface groups (perruthenate in this case), which may occur via interfacial cyclic redox catalysis and constitutes electrocatalytic mechanism [27].

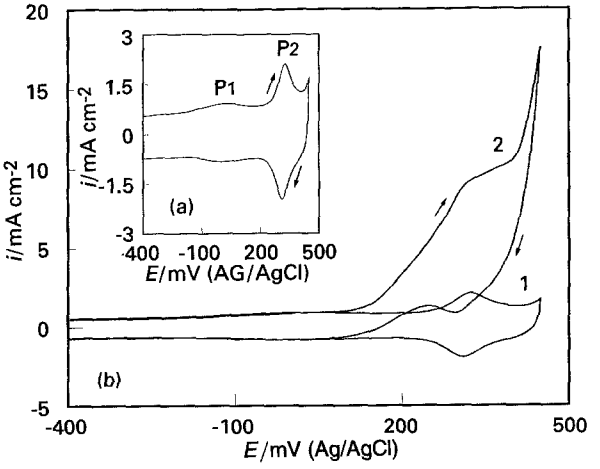

Fig. 1. (a) Cyclic voltammogram of a RuO_2 electrode in 1 M KOH; (b) Cyclic voltammogram of a RuO_2 electrode in (1) 1 M KOH; (2) 1 M KOH + 0.3 M benzyl alcohol, with a scan rate of 50 mV s^{-1}.

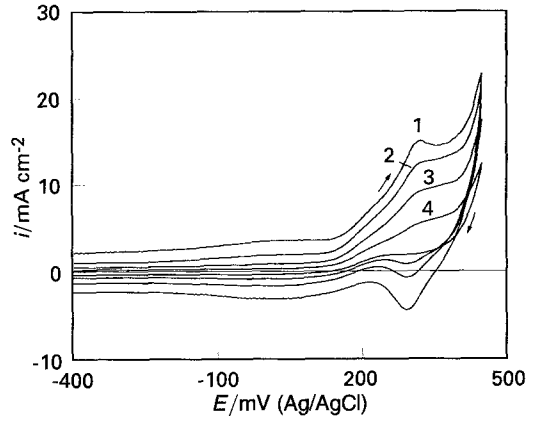

Fig. 2. Voltammetric curves of the oxidation of benzyl alcohol on a RuO_2 electrode in 1 M KOH containing 0.3 M benzyl alcohol for the following scan rates: (1) 200, (2) 100, (3) 50, and (4) 20 mV s^{-1}.

The CV diagrams, run at different scan rates for the RuO_2 electrode in 1 M KOH containing 0.3 M benzyl alcohol, are presented in Fig. 2. Figure 2 shows that the currents of curves 3 and 4 in the 150–400 mV potential range for both the anodic and cathodic sweeps are positive; while in curves 1 and 2, although the anodic current is larger, a cathodic peak corresponding to Ru(VII)/Ru(VI) transition is observed. This shows that the rate of reaction between the benzyl alcohol and the perruthenate is slower than that of electrochemical reaction involving the oxidation of Ru(VI) to Ru(VII) on the time scale of the higher scan rates such as 100 mV s^{-1}; revealing that the heterogeneous oxidation of benzyl alcohol on RuO_2 electrode is not a fast reaction. Therefore, the rate-determining step for benzyl alcohol oxidation on a RuO_2 electrode is thought to be the chemical reaction between the surface perruthenate species and the organic species, rather than the formation of perruthenate from ruthenate.

3.2. *Kinetic studies*

Figure 3 shows the Tafel plots obtained under quasi-steady state conditions for the oxidation of various benzyl alcohol concentrations. The Tafel plots were

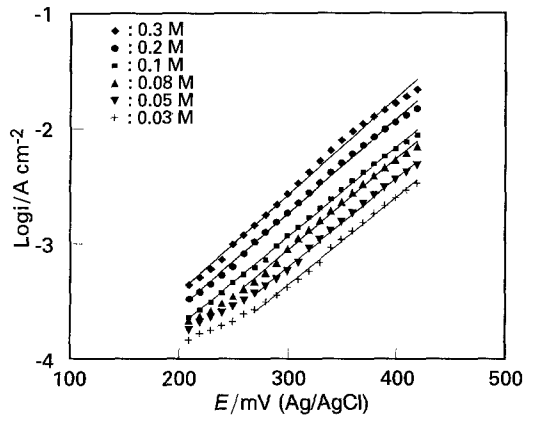

Fig. 3. Tafel plots at various benzyl alcohol concentrations in 1 M KOH solution with a scan rate of 1 mV s^{-1} at 25° C. Concentrations: (◆) 0.3, (●) 0.2, (■) 0.1, (▲) 0.08, (▼) 0.05 and (+) 0.03 M.

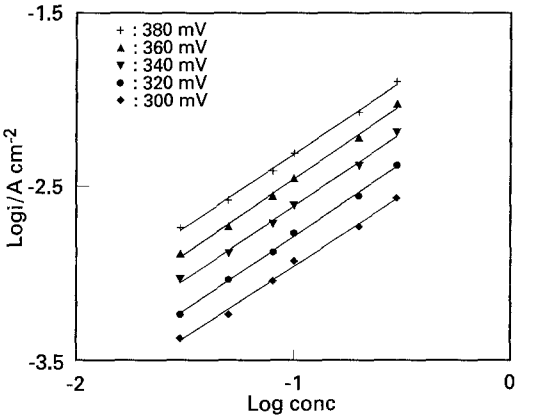

Fig. 4. A double logarithmic plot of current density as a function of benzyl alcohol concentrations at constant electrode potentials. Conditions as in Fig. 3. Potentials: (+) 380, (▲) 360, (▼) 340, (●) 320 and (◆) 300 mV.

obtained at a scan rate of 1 mV s^{-1} in 1 M KOH solution. There is no significant change in the slope with varying benzyl alcohol concentration and the average value obtained is 125 ± 4 mV per current decade. The value of the product of the transfer coefficient and the electrons transferred (αn) is 0.47.

A logarithmic plot of the current density as a function of benzyl alcohol concentration at constant electrode potential is shown in Fig. 4. From the slope of the curves, a reaction order of ca. 0.85 is found for the anodic oxidation of benzyl alcohol on RuO_2 and this is independent of potential in the range of exploration.

Figure 5 shows the Tafel plots as a function of pH obtained under the same conditions as above for a benzyl alcohol concentration of 0.1 M at 25° C. The Tafel slope obtained in this pH range decreases slightly with increasing pH value (from 126 to 114 mV) and the average value is 120 mV. This value is comparable with that calculated from the Tafel plots at different concentrations (Fig. 3). At higher pH and higher anodic potential, a nonlinear $\log i/E$ plot is observed (for example, ca. 300 mV at pH 14.25). This indicates that, at higher pH, the rate of oxidation of benzyl alcohol on RuO_2 electrode gradually approaches the rate of its transport to the electrode.

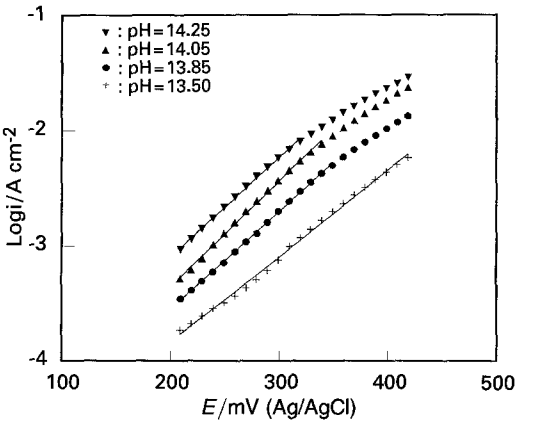

Fig. 5. Tafel plots at various KOH concentrations containing 0.1 M benzyl alcohol with a scan rate of 1 mV s^{-1} at 25° C. pH: (▼) 14.25, (▲) 14.05, (●) 13.85 and (+) 13.50.

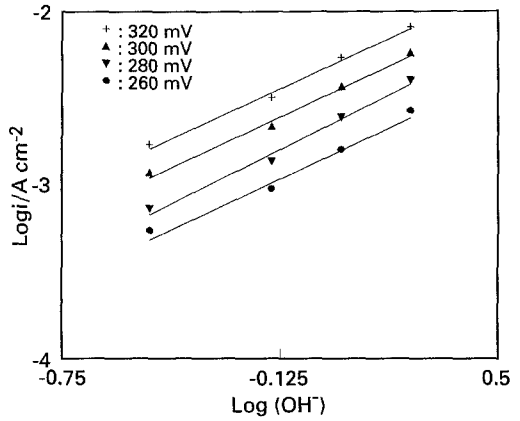

Fig. 6. A double logarithmic plot of current density as a function of KOH concentration at constant electrode potentials. Conditions as in Fig. 5. Potentials: (+) 320, (▲) 300, (▼) 280 and (●) 260 mV.

A logarithmic plot of the current density as a function of OH^- concentration at constant electrode potential is shown in Fig. 6. The plot is linear with a slope of 0.96, suggesting a reaction order of unity with respect to OH^-.

The dependence of the Tafel plots on temperature was also examined in 1 M KOH solution containing 0.3 M benzyl alcohol for various temperatures in the range 25–75° C. A constant Tafel slope of ca. 120 mV was obtained in the above temperature range. Log i against T^{-1} plots at constant electrode potential are shown in Fig. 7. From the slope of the Arrhenius lines, an activation energy of $34.4 \pm 0.5\,kJ\,mol^{-1}$ for chemical reaction between benzyl alcohol and surface perruthenate species is obtained, which also supports the previous suggestion on the cyclic voltammetric results that the breaking of a chemical bond is the rate-determining step.

Based on the above results, a reaction scheme may be tentatively outlined for the oxidation of benzyl alcohol on RuO_2, where perruthenate (Ru(VII)) species, electrogenerated at the anode surface, catalyse the benzyl alcohol oxidation.

$$RuO_4^{2-} \overset{k_e}{\rightleftharpoons} RuO_4^- + e^- \qquad (2)$$

$$[C_6H_5CH_2OH]_{sol} \xrightarrow{k_{ads}} [C_6H_5CH_2OH]_{ads} \qquad (3)$$

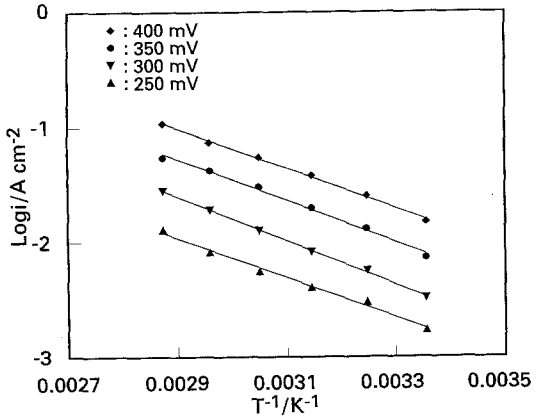

Fig. 7. Dependence of log i on T^{-1} at constant electrode potentials. Experimental conditions: 0.3 M benzyl alcohol in 1 M KOH solution; scan rate = $1\,mV\,s^{-1}$. Potentials: (◆) 400, (●) 350, (▼) 300 and (▲) 250 mV.

$$[C_6H_5CH_2OH]_{ads} + OH^- + RuO_4^- \xrightarrow{k_c} [C_6H_5\dot{C}HOH] + RuO_4^{2-} + H_2O \qquad (4)$$

$$[C_6H_5\dot{C}HOH] \longrightarrow \text{Products} \qquad (5)$$

Equations 2 and 3 represent the electrochemical reaction involving the formation of perruthenate from ruthenate in a thin hydrated layer at the oxide-solution interface, and the adsorption of benzyl alcohol on the RuO_2 electrode, respectively. Equation 4 represents the chemical reaction, abstracting hydrogen from the α-carbon of the alcohol by perruthenate species, which is thought to be the rate-determining step in the overall reaction scheme. The above proposed reaction mechanism is similar to that in previous work in a similar reaction system, alcohol oxidation at oxide-covered anodes [2].

The observed fractional reaction order (0.85) with respect to benzyl alcohol concentration, in addition to the literature evidence [1, 2, 12, 13, 23] indicates that the adsorption of organic species is necessary prior to the chemical reaction (Equation 3) in a heterogeneous system. Any reaction mechanism where the organic species adsorbs on the surface of the lower oxide state and reacts with an adjacent perruthenate species would lead to a large and pronounced current maximum in the i/E curve (at high overpotential, the active sites are completely transformed into perruthenate and as a consequence, the coverage by the organic compound falls sharply). Since such maxima are not observed (see Figs 1 and 2), the adsorption must be on the surface of the higher oxide state and the chemical reaction occurs directly at the adsorbed organic species and the active site with the incorporation of a hydroxyl ion from the neighbouring reaction layer.

3.3. *Determination of final products*

The galvanostatic electrolysis results show that the products of benzyl alcohol oxidation of the RuO_2 electrode are benzaldehyde and benzoic acid. As a consequence, a possible reaction scheme for the transformation of the intermediate radical ($C_6H_5\dot{C}HOH$) to the corresponding products may be formulated as follows, as is well recognized in the radical type reaction mechanism for alcohol oxidation [2, 4].

$$[C_6H_5\dot{C}HOH] + OH^- \xrightarrow{k_1} [C_6H_5COH] + H_2O + e^- \qquad (6)$$

$$[C_6H_5\dot{C}HOH] + 3OH^- \xrightarrow{k_2} [C_6H_5COOH] + 2H_2O + 3e^- \qquad (7)$$

From Equations 6 and 7, the selectivity depends on the environment of the electrolytic solution. Therefore, the effect of such electrolytic conditions as t-butanol (t-BuOH) concentration, current density, OH^- concentration, and temperature on the benzyl alcohol oxidation current efficiency and benzaldehyde selectivity was studied.

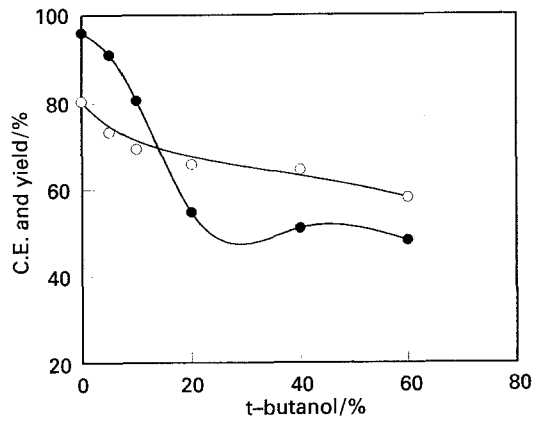

Fig. 8. Effect of *t*-BuOH concentrations on current efficiency and benzaldehyde selectivity; (●) current efficiency; (○) benzaldehyde selectivity. Electrolytic conditions: 0.3 M benzyl alcohol in 1 M KOH solution; current density 5 mA cm^{-1}; charge passed 0.5 F mol^{-1} at 25° C.

3.3.1. Effect of t-*BuOH concentration.* The dependence of benzyl alcohol oxidation current efficiency and benzaldehyde production selectivity on *t*-BuOH concentration in 1 M KOH solution containing 0.3 M benzyl alcohol are plotted in Fig. 8. An examination of Fig. 8 reveals that, for *t*-BuOH concentration < 20%, the benzyl alcohol oxidation current efficiency substantially decreases with increasing *t*-BuOH concentration (from 96 to ca. 50%). For *t*-BuOH concentration > 20%, however, the current efficiency becomes independent of cosolvent concentration. In the case of the electrolyte without organic solvent (*t*-BuOH), a visible organic layer adsorbed on the RuO_2 electrode was observed in the course of galvanostatic electrolysis. This is also suggested by the increase in electrode potential during galvanostatic electrolysis at a constant current density of 5 mA cm^{-2} (curve 1 in Fig. 9). From curve 1 in Fig. 9, for charge passed < 0.1 F mol^{-1}, the electrode potential is observed to increase substantially from 420 to 570 mV. For charge passed > 0.1 F mol^{-1}, however, the increase in electrode potential decreases and the electrode potential reaches a constant value at ca. 640 mV after 0.4 F mol^{-1} charge passed. The former result suggests that the substrate/products are easily adsorbed and continuously accumulate at the electrode surface during electrolysis, which increases the electrode resistance; the latter result indicates that the adsorption tends to be saturated after 0.4 F mol^{-1} charge passed. In comparison to curve 2 in Fig. 9, although the potential in curve (·) is higher after 0.1 F mol^{-1} charge, the current efficiency for benzyl alcohol oxidation is higher in aqueous solution (96 as compared to 50% for benzyl alcohol oxidation in 20% *t*-BuOH electrolytic solution). This clearly demonstrates that, in aqueous solution, adsorption of organic substances increases the hydrophobicity of the anode surface and, consequently, enhances the interaction between benzyl alcohol and the RuO_2 electrode, resulting in the observed high current efficiency.

Figure 8 also shows that the benzaldehyde selectivity decreases with increasing *t*-BuOH concentration (from 81 to 58%). This result is significantly different from that for benzyl alcohol oxidation on nickel hydroxide (NiOOH). In an aqueous solution, the major product of benzyl alcohol oxidation on nickel hydroxide was benzoic acid; while, in mixed organic solvents, or in emulsion electrolysis, the major product was benzaldehyde [3, 4]. This indicates that the stability to adsorption/desorption of substrate/product on RuO_2 was different from that on nickel. The strong adsorption of aromatic organics on RuO_2 increases the hydrophobicity of the anode surface and, consequently, decreases the possibility of OH^- in contact with the electrode. Accordingly, the yield of benzoic acid was significantly lower in this case (cf. Equations 6 and 7). However, the interaction between benzyl alcohol and the anode surface is weakened at high *t*-BuOH concentration, which decreases the hydrophobicity of the anode surface and, consequently, increases the possibility of OH^- in contact with the electrode. Under such circumstance, the yield of benzoic acid is increased (cf. Equations 6 and 7).

3.3.2. Effect of current density. Figure 10 shows the dependence of current efficiency and benzaldehyde

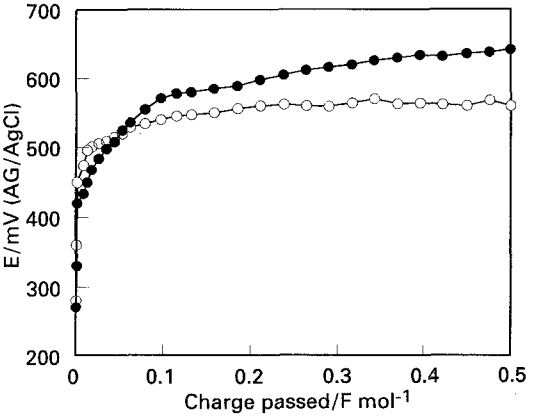

Fig. 9. Dependence of electrode potential for benzyl alcohol oxidation on the amount of passed charge. Electrolytic conditions: (●) 0.3 M benzyl alcohol in 1 M KOH; (○) 0.3 M benzyl alcohol in 1 M KOH + 20% *t*-BuOH; current density 5 mA cm^{-1} at 25° C.

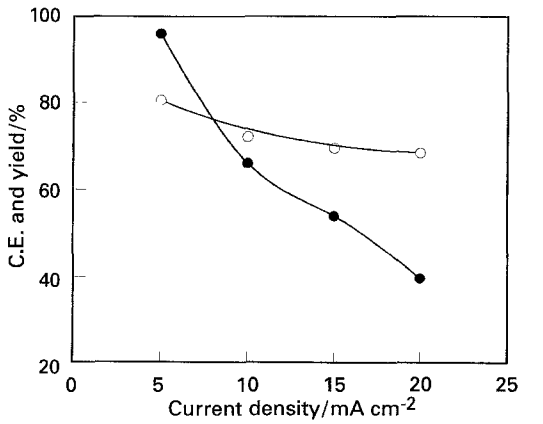

Fig. 10. Effect of current density on current efficiency and benzaldehyde selectivity; (●) current efficiency; (○) benzaldehyde selectivity. Electrolytic conditions: 0.3 M benzyl alcohol in 1 M KOH solution; charge passed 0.5 F mol^{-1} at 25° C.

selectivity on electrolysis current density. The current efficiency is strongly affected by current density; as current density increases from 5 to 20 mA cm^{-2}, the current efficiency decreases from 96 to 40%. This can be explained by the fact that, at higher current density, competitive oxygen evolution occurs. In addition, benzaldehyde selectivity also decreases with increasing current density (from 80 to ca. 70%).

3.3.3. Effect of OH^- concentration. The dependence of benzyl alcohol oxidation current efficiency and benzaldehyde selectivity on OH^- concentration (Fig. 11) shows that the current efficiency increases linearly with increasing OH^- concentration, while the benzaldehyde selectivity decreases. These results lend further support to the reaction scheme proposed (cf. Equations 4, 6 and 7). Examination of Equation 4 reveals that the reaction rate between benzyl alcohol and perruthenate increases with increasing OH^- concentration and, consequently, increases the current efficiency. A comparison of Equations 6 and 7, on the other hand, reveals that at higher OH^- concentration, the rate of increase in benzoic acid yield (Equation 7) would be higher than that of increase in benzaldehyde yield (Equation 6); this results in the observed lower benzaldehyde selectivity.

3.3.4. Effect of temperature. Figure 12 shows that although the current efficiency increases with increasing electrolysis temperature, benzaldehyde selectivity is independent of temperature. The former result indicates that the rate of increase in chemical reaction rate between perruthenate and benzyl alcohol with increasing temperature is higher than that of the increase in oxygen evolution rate.

4. Conclusions

The oxidation of benzyl alcohol on RuO_2 electrodes commences at a potential where an oxidizing surface oxyruthenium species (perruthenate) is electrogenerated. This electrogenerated surface perruthenate species oxidizes the benzyl alcohol in a heterogeneous manner via an interfacial cyclic redox catalysis process in a thin hydrated layer at the oxide-solution interface. The reaction orders with respect to benzyl alcohol and OH^- concentrations are 0.85 and 1, respectively. The fractional reaction order (0.85) with respect to benzyl alcohol bulk concentration is indicative of the adsorption of benzyl alcohol on the RuO_2 electrode. The galvanostatic electrolysis results show that the current efficiency for benzyl alcohol oxidation decreases with increasing *t*-BuOH concentration and current density, and increases with increasing OH^- concentration and temperature, while the benzaldehyde selectivity decreases with increasing *t*-BuOH concentration, current density and OH^- concentration, and is independent of temperature.

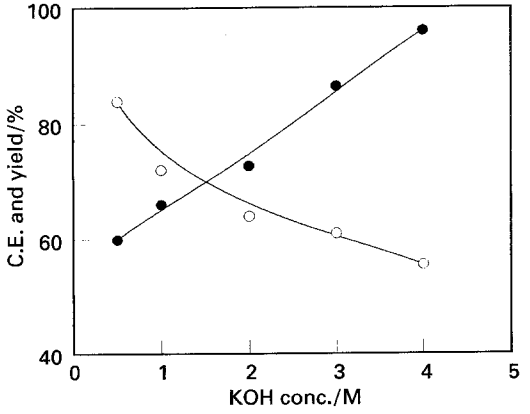

Fig. 11. Effect of KOH concentrations on current efficiency and benzaldehyde selectivity; (●) current efficiency; (○) benzaldehyde selectivity. Electrolytic conditions: 0.3 M benzyl alcohol; current density 10 mA cm^{-1}; charge passed 0.5 F mol^{-1} at 25° C.

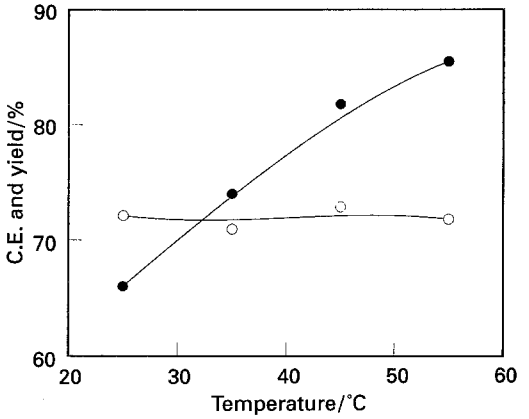

Fig. 12. Effect of temperature on current efficiency and benzaldehyde selectivity; (●) current efficiency; (○) benzaldehyde selectivity. Electrolytic conditions: 0.3 M benzyl alcohol in 1 M KOH; current density 10 mA cm^{-1}; charge passed 0.5 F mol^{-1}.

Acknowledgements

The financial support of this work by the National Science Council of the Republic of China under contract NSC 83-0402-E006-055, is gratefully acknowledged.

References

[1] M. Fleischmann, K. Korinek and D. Pletcher, *J. Electroanal. Chem.* **31** (1971) 39.
[2] *Idem, J. Chem. Soc., Perkins Trans. II* (1972) 1396.
[3] M. Amjad, D. Pletcher and C. Smith, *J. Electrochem. Soc.* **124** (1977) 203.
[4] H. J. Schäfer, *Topics in Current Chemistry* **142** (1986) 101.
[5] F. Beck and H. Schulz, *Electrochim. Acta* **29** (1984) 1569.
[6] *Idem, J. Electroanal. Chem.* **229** (1987) 339.
[7] *Idem, J. Appl. Electrochem.* **17** (1987) 914.
[8] H. Schulz and F. Beck, *Angew. Chem. Int. Ed. Engl.* **24** (1985) 1049.
[9] C. Ravichandran, D. Vasudevan and P. N. Anantharaman, *J. Appl. Electrochem.* **22** (1992) 1192.
[10] C. Ravichandran, D. Vasudevan, S. Thangavela and P. N. Anantharaman, *ibid.* **22** (1992) 1087.
[11] C. Ravichandran, D. Vasudevan and P. N. Anantharaman, *ibid.* **22** (1992) 179.
[12] A. M. Couper, D. Pletcher and F. C. Walsh, *Chem. Rev.* **90** (1990) 837.
[13] D. Pletcher, *J. Appl. Electrochem.* **14** (1984) 403.
[14] Electrodes of Conductive Metallic Oxides, Part A (edited by S. Trasatti), Elsevier, Amsterdam (1980).

[15] Electrodes of Conductive Metallic Oxides, Part B (edited by S. Trasatti), Elsevier, Amsterdam (1981).
[16] S. M. Lin and T. C. Wen, *J. Electrochem. Soc.* **140** (1993) 2265.
[17] T. C. Wen and C. C. Hu, *ibid.* **139** (1992) 2158.
[18] E. J. M. O'Sullivan and J. R. White, *ibid.* **136** (1989) 2576.
[19] M. E. G. Lyons, C. H. Lyons, A. Michas and P. N. Bartlett, *J. Electroanal. Chem.* **351** (1993) 245.
[20] S. Cosnier, A. Deronzier and J. F. Roland, *J. Molecular Catalysis* **71** (1992) 303.
[21] S. Cosnier, A. Deronzier and J. C. Moutet, *Inorg. Chem.* **27** (1988) 2390.
[22] S. M. Lin and T. C. Wen, *Electrochim. Acta* **39** (1994) 393.
[23] B. E. Conway, *J. Molecular Catalysis* **54** (1989) 353.
[24] L. D. Burke and J. F. Healy, *J. Electroanal. Chem.* **124** (1981) 327.
[25] S. Ardizzone, A. Daghetti, L. Franceschi and S. Trasatti, *Colloids and Surfaces* **35** (1989) 85.
[26] M. E. G. Lyons and L. D. Burke, *J. Chem. Soc. Faraday Trans. I* **83** (1987) 299.
[27] A. R. Hillmam, *in* 'Electrochemical Science and Technology of Polymers – I', (edited by R. G. Linford), Elsevier, London (1987) pp. 103–291.